

## **Forsmark site investigation**

### **Geological single-hole interpretation of KFM08D**

Seje Carlsten, Eva Samuelsson  
Geosigma AB

Jaana Gustafsson, Malå GeoScience AB

Michael Stephens, Geological Survey of Sweden

Hans Thunehed, GeoVista AB

October 2007

**Svensk Kärnbränslehantering AB**

Swedish Nuclear Fuel  
and Waste Management Co  
Box 5864  
SE-102 40 Stockholm Sweden  
Tel 08-459 84 00  
+46 8 459 84 00  
Fax 08-661 57 19  
+46 8 661 57 19



## **Forsmark site investigation**

# **Geological single-hole interpretation of KFM08D**

Seje Carlsten, Eva Samuelsson  
Geosigma AB

Jaana Gustafsson, Malå GeoScience AB

Michael Stephens, Geological Survey of Sweden

Hans Thunehed, GeoVista AB

October 2007

*Keywords:* Forsmark, Geophysics, Geology, Borehole, Bedrock, Fractures,  
AP PF 400-07-017.

This report concerns a study which was conducted for SKB. The conclusions and viewpoints presented in the report are those of the authors and do not necessarily coincide with those of the client.

Data in SKB's database can be changed for different reasons. Minor changes in SKB's database will not necessarily result in a revised report. Data revisions may also be presented as supplements, available at [www.skb.se](http://www.skb.se).

A pdf version of this document can be downloaded from [www.skb.se](http://www.skb.se).

# Abstract

This report presents a geological single-hole interpretation of the cored borehole KFM08D at Forsmark. The interpretation combines the geological core mapping, generalized geophysical logs and borehole radar measurements to identify where rock units and possible deformation zones occur in the boreholes. A brief description of the character of each rock unit and possible deformation zone is provided.

The geological single-hole interpretation shows that five rock units (RU1–RU5) occur in KFM08D. However, the borehole can be divided into nine separate sections due to the repetition of RU2 (RU2a, RU2b and RU2c), RU3 (RU3a and RU3b) and RU4 (RU4a and RU4b).

Medium-grained metagranite-granodiorite (101057) dominates in rock units RU1 and RU2. These units are distinguished solely on the basis of the common occurrence of albitization of the granite in RU2. Pegmatitic granite (101061), fine- to medium-grained metagranitoid (101051) and amphibolite (102017) are subordinate rock types in both RU1 and RU2. Amphibolite (102017), metadiorite (101033) and pegmatitic granite (101061) dominate in rock unit RU3. A heterogeneous unit with fine- to medium-grained metagranitoid (101051), which is inferred to be tonalitic in composition on the basis of the silicate density, pegmatitic granite (101061) and medium-grained metagranite-granodiorite (101057) is present in RU4. The subordinate rock types fine- to medium-grained granite (111058) and felsic to intermediate metavolcanic rock (103076) are also present. Fine- to medium-grained metagranitoid (101051), which is inferred to be granodioritic to tonalitic in composition, dominates rock unit RU5. Albitization affects subordinate medium-grained metagranite-granodiorite and pegmatitic granite in RU4 and RU5.

Twelve possible deformation zones, which predominantly show an increased frequency of sealed fractures, have been identified in KFM08D (DZ1–DZ12).

## Sammanfattning

Denna rapport behandlar geologisk enhålstolkning av kärnborrhål KFM08D i Forsmark. Den geologiska enhålstolkningen syftar till att utifrån den geologiska karteringen, tolkade geofysiska loggar och borrhålsradarmätningar indikera olika litologiska enheters fördelning i borrhålen samt möjliga deformationszoners läge och utbredning. En kort beskrivning av varje bergenhets och möjlig deformationszon presenteras.

Denna undersökning visar att det i KFM08D finns fem litologiska enheter (RU1–RU5). Baserat på repetition av enheterna RU2 (RU2a, RU2b och RU2c), RU3 (RU3a och RU3b) och RU4 (RU4a och RU4b) kan borrhålet delas in i nio sektioner.

Medelkornig metagranit-granodiorit (101057) dominerar de litologiska enheterna RU1 och RU2. Dessa enheter urskiljs enbart genom en generell förekomst av albitisering av graniten i RU2. Pegmatitisk granit (101061), fin- till medelkornig metagranitoid (101051) och amfibolit (102017) utgör underordnade bergarter i både RU1 och RU2. Amfibolit (102017), metadiorit (101033) och pegmatitisk granit (101061) dominerar den litologiska enheten RU3. En heterogen enhet bestående av fin- till medelkornig metagranitoid (101051), vilken, grundat på silikatdensiteten, tolkas vara tonalitisk i sammansättningen, pegmatitisk granit (101061) och medelkornig metagranit-granodiorit (101057) utgör RU4. De underordnade bergarterna fin- till medelkornig granit (111058) och felsisk till intermediär metavulkanisk bergart (103076) förekommer även. Fin- till medelkornig metagranitoid (101051), vilken är tolkad till granodioritisk till tonalitisk i sammansättning, dominerar den litologiska enheten RU5. Albitisering påverkar underordnad medelkornig metagranit-granodiorit och pegmatitisk granit i RU4 och RU5.

Tolv möjliga deformationszoner, vilka huvudsakligen uppvisar en förhöjd frekvens av läkta sprickor, har identifierats i KFM08D (DZ1–DZ12).

# Contents

<b>1</b>	<b>Introduction</b>	7
<b>2</b>	<b>Objective and scope</b>	9
<b>3</b>	<b>Data used for the geological single-hole interpretation</b>	11
<b>4</b>	<b>Execution of the geological single-hole interpretation</b>	15
4.1	General	15
4.2	Nonconformities	18
<b>5</b>	<b>Results</b>	19
5.1	KFM08D	19
<b>6</b>	<b>Comments</b>	23
	<b>References</b>	25
<b>Appendix 1</b>	<b>Geological single-hole interpretation of KFM08D</b>	27

# 1 Introduction

Much of the primary geological and geophysical borehole data stored in the SKB database SICADA need to be integrated and synthesized before they can be used for modelling in the 3D-CAD Rock Visualization System (RVS). The end result of this procedure is a geological single-hole interpretation, which consists of an integrated series of different logs and accompanying descriptive documents.

This document reports the geological single-hole interpretation of borehole KFM08D in the Forsmark area. The horizontal projection of the borehole is shown in Figure 1-1. The work was carried out in accordance with activity plan AP PF 400-07-017. The controlling documents for performing this activity are listed in Table 1-1. Both the activity plan and method description are SKB's internal controlling documents.

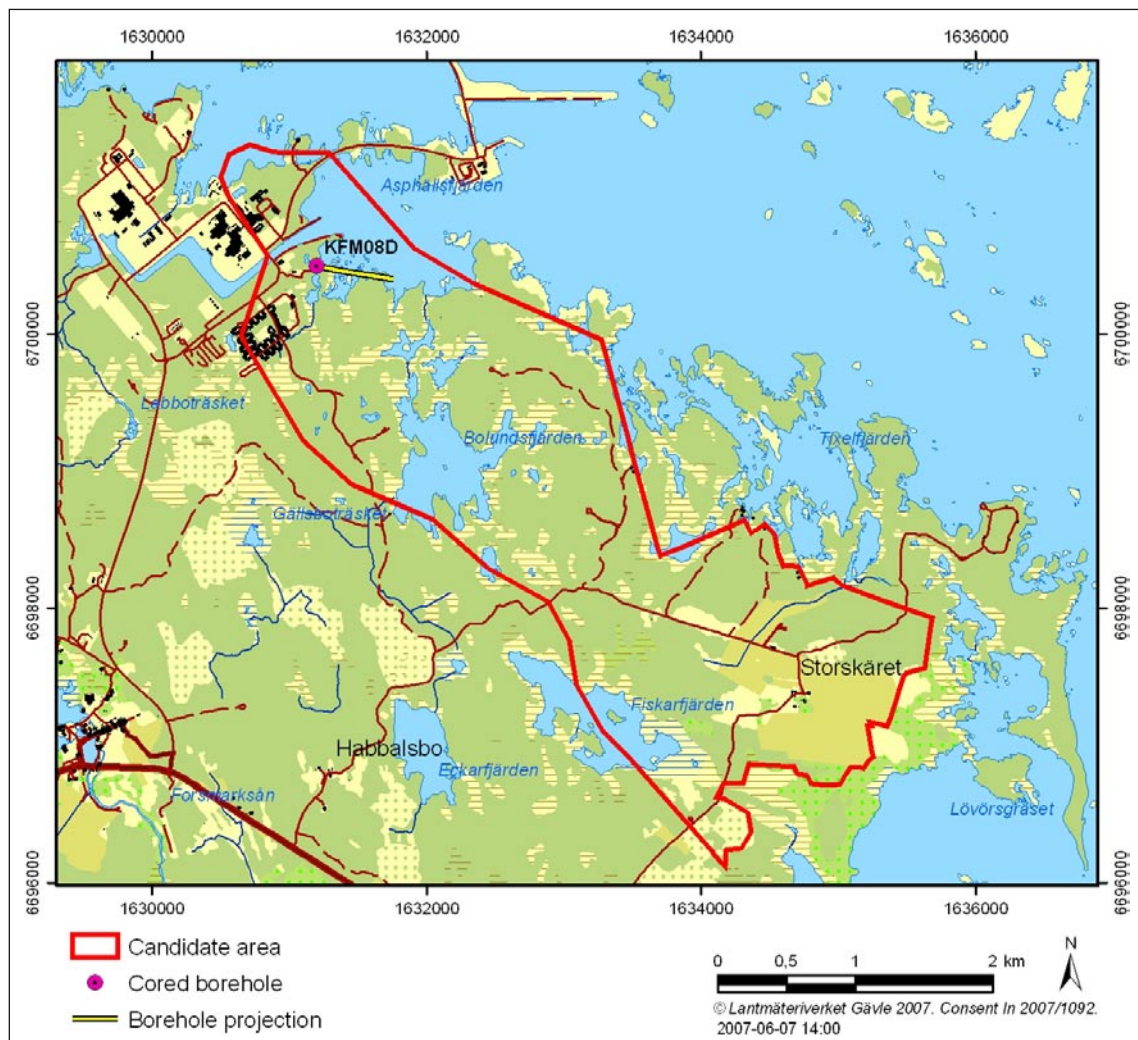


Figure 1-1. Map showing position and horizontal projection of the cored borehole KFM08D.

Original data from the reported activity are stored in the primary database Sicada, where they are traceable by the Activity Plan number (AP PF 400-07-017). Only data in SKB's databases are accepted for further interpretation and modelling. The data presented in this report are regarded as copies of the original data. Data in the databases may be revised, if needed. Such revisions will not necessarily result in a revision of the P-report, although the normal procedure is that major data revisions entail a revision of the P-report. Minor data revisions are normally presented as supplements, available at [www.skb.se](http://www.skb.se).

**Table 1-1. Controlling documents for the performance of the activity**

<b>Activity plan</b>	<b>Number</b>	<b>Version</b>
Geologisk enhålstolkning av KFM08D	AP PF 400-07-017	1.0
<b>Method description</b>	<b>Number</b>	<b>Version</b>
Metodbeskrivning för geologisk enhålstolkning	SKB MD 810.003	3.0

## 2 Objective and scope

A geological single-hole interpretation is carried out in order to identify and to describe briefly the characteristics of major rock units and possible deformation zones within a borehole. The work involves an integrated interpretation of data from the geological mapping of the borehole (Boremap), different borehole geophysical logs and borehole radar data.

The geological mapping of the cored borehole involves a documentation of the character of the bedrock in the drill core. This work component is carried out in combination with an inspection of the oriented image of the borehole walls that is obtained with the help of the *Borehole Image Processing System (BIPS)*. The interpretations of the borehole geophysical and radar logs are available when the single-hole interpretation is completed. The result from the geological single-hole interpretation is presented in a WellCad plot. A more detailed description of the technique is provided in the method description for geological single-hole interpretation (SKB MD 810.003, internal document). The work reported here concerns stage 1 in the single-hole interpretation, as defined in the method description.



### 3 Data used for the geological single-hole interpretation

The following data and interpretations have been used for the single-hole interpretation of the borehole KFM08D:

- Boremap data (including BIPS and geological mapping data) /3/.
- Generalized geophysical logs and their interpretation /4/.
- Radar data and their interpretation /5/.

The material used as a basis for the geological single-hole interpretation was a WellCad plot consisting of parameters from the geological mapping in the Boremap system, geophysical logs and borehole radar. An example of a WellCad plot used during geological single-hole interpretation is shown in Figure 3-1. The plot consists of ten main columns and several subordinate columns. These include:

- 1: Length along the borehole
- 2: Rock type
  - 2.1: Rock type
  - 2.2: Rock type structure
  - 2.3: Rock type texture
  - 2.4: Rock type grain size
  - 2.5: Structure orientation
  - 2.6: Rock occurrence (< 1 m)
  - 2.7: Rock alteration
  - 2.8: Rock alteration intensity
- 3: Unbroken fractures
  - 3.1: Primary mineral
  - 3.2: Secondary mineral
  - 3.3: Third mineral
  - 3.4: Fourth mineral
  - 3.5: Alteration, dip direction
- 4: Broken fractures
  - 4.1: Primary mineral
  - 4.2: Secondary mineral
  - 4.3: Third mineral
  - 4.4: Fourth mineral
  - 4.5: Aperture (mm)
  - 4.6: Roughness
  - 4.7: Surface
  - 4.8: Alteration, dip direction
- 5: Crush zones
  - 5.1: Primary mineral
  - 5.2: Secondary mineral
  - 5.3: Third mineral
  - 5.4: Fourth mineral
  - 5.5: Roughness
  - 5.6: Surface
  - 5.7: Crush alteration, dip direction
  - 5.8: Piece (mm)
  - 5.9: Sealed network
  - 5.10: Core loss

- 6: Fracture frequency
  - 6.1: Open fractures
  - 6.2: Sealed fractures
- 7: Geophysics
  - 7.1: Magnetic susceptibility
  - 7.2: Natural gamma radiation
  - 7.3: Possible alteration
  - 7.4: Silicate density
  - 7.5: Estimated fracture frequency
- 8: Radar
  - 8.1: Length
  - 8.2: Angle
- 9: Reference mark (not used for percussion-drilled boreholes)
- 10: BIPS

The geophysical logs are described below:

*Magnetic susceptibility:* The rock has been classified into sections of low, medium, high, and very high magnetic susceptibility. The susceptibility measurement is strongly connected to the magnetite content in the different rock types.

*Natural gamma radiation:* The rock has been classified into sections of low, medium, and high natural gamma radiation. Low radiation may indicate mafic rock types and high radiation may indicate younger, fine-grained granite or pegmatite. The rocks with high natural gamma radiation have been included in the younger, Group D intrusive suite /1/.

*Possible alteration:* This parameter has not been used in the geological single-hole interpretation in the Forsmark area.

*Silicate density:* This parameter indicates the density of the rock after subtraction of the magnetic component in the rock. It provides general information on the mineral composition of the rock types, and serves as a support during classification of rock types.

*Estimated fracture frequency:* This parameter provides an estimate of the fracture frequency along 5 m sections, calculated from short and long normal resistivity, SPR, P-wave velocity as well as focused resistivity 140 and 300. The estimated fracture frequency is based on a statistical connection after a comparison has been made between the geophysical logs and the mapped fracture frequency. The log provides an indication of sections with low and high fracture frequencies.

Close inspection of the borehole radar data was carried out during the interpretation process, especially during the identification of possible deformation zones. The occurrence and orientation of radar anomalies within the possible deformation zones are commented upon in the text that describes these zones.



## 4 Execution of the geological single-hole interpretation

### 4.1 General

The geological single-hole interpretation has been carried out by a group of geoscientists consisting of both geologists and geophysicists. Several of these geoscientists previously participated in the development of the source material for the single-hole interpretation. All data to be used (see Chapter 3) are visualized side by side in a borehole document extracted from the software WellCad. The working procedure is summarized in Figure 4-1 and in the text below.

The first step in the working procedure is to study all types of data (rock type, rock alteration, silicate density, natural gamma radiation, etc) related to the character of the rock type and to merge sections of similar rock types, or sections where one rock type is very dominant, into rock units (minimum length of c 5 m). Each rock unit is defined in terms of the borehole length interval and provided with a brief description for inclusion in the WellCad plot. The confidence in the interpretation of a rock unit is made on the following basis: 3 = high, 2 = medium and 1 = low.

The second step in the working procedure is to identify possible deformation zones by visual inspection of the results of the geological mapping (fracture frequency, fracture mineral, aperture, alteration, etc) in combination with the geophysical logging and radar data. The section of each identified possible deformation zone is defined in terms of the borehole length interval and provided with a brief description for inclusion in the WellCad plot. This includes a brief description of the rock types affected by the possible deformation zone. The confidence in the interpretation of a possible deformation zone is made on the following basis: 3 = high, 2 = medium and 1 = low.

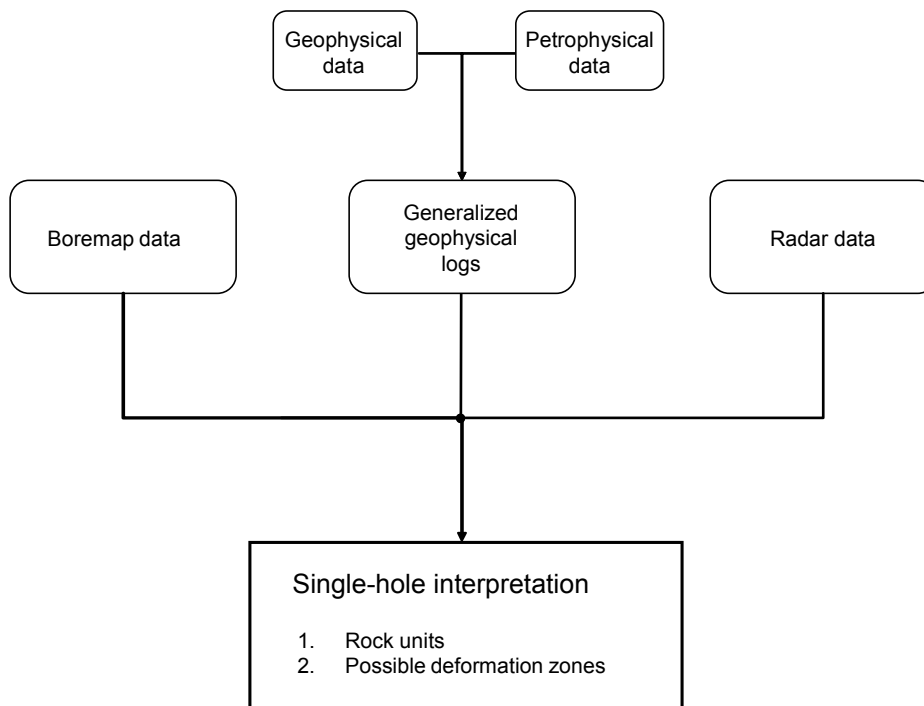


**Figure 4-1.** Schematic chart that shows the procedure for the development of a geological single-hole interpretation.

Inspection of BIPS images is carried out wherever it is judged necessary during the working procedure. Furthermore, following definition of rock units and possible deformation zones, with their respective confidence estimates, the drill cores are inspected in order to check the selection of the boundaries between these geological entities. If judged necessary, the location of these boundaries is adjusted.

Possible deformation zones that are brittle in character have been identified primarily on the basis of the frequency of fractures, according to the concept presented in /2/. Brittle deformation zones defined by an increased fracture frequency of extensional fractures (joints) or shear fractures (faults) are not distinguished. Both the transitional part, with a fracture frequency in the range 4–9 fractures/m, and the core part, with a fracture frequency > 9 fractures/m, have been included in each zone (Figure 4-2). The frequencies of open and sealed fractures have been assessed in the identification procedure, and the character of the zone has been described accordingly. Partly open fractures are included together with open fractures in the brief description of each zone. The presence of bedrock alteration, the occurrence and, locally, inferred orientation of radar reflectors, the resistivity, SPR, P-wave velocity, caliper and magnetic susceptibility logs have all assisted in the identification of the zones. The anomalies in these parameters that assist with the identification are presented in the short description.

Since the frequency of fractures is of key importance for the definition of the possible deformation zones, moving average plots for this parameter are shown for the cored bore-hole KFM08D (Figure 4-3). A 5 m window and 1 m steps have been used in the calculation procedure. The moving average for open fractures alone, the total number of open fractures (open, partly open and crush), the sealed fractures alone, and the total number of sealed fractures (sealed and sealed fracture network) are shown in a diagram.

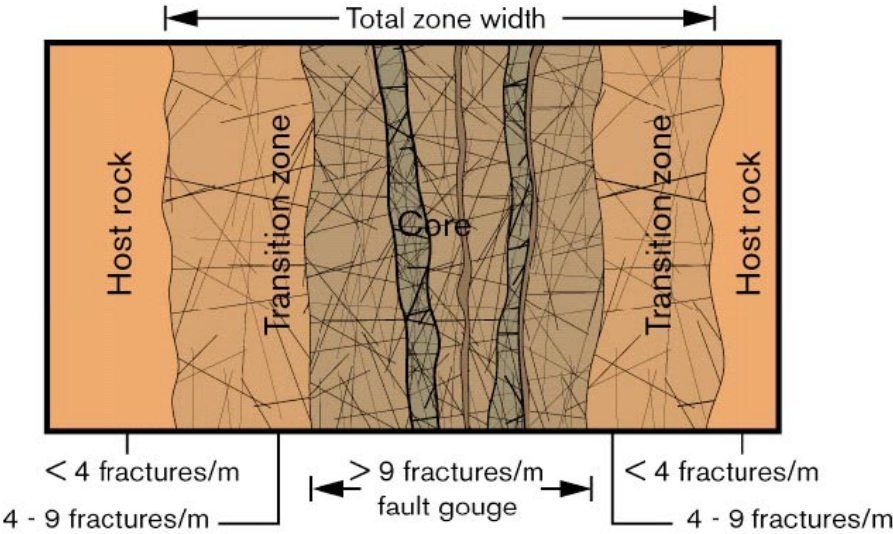
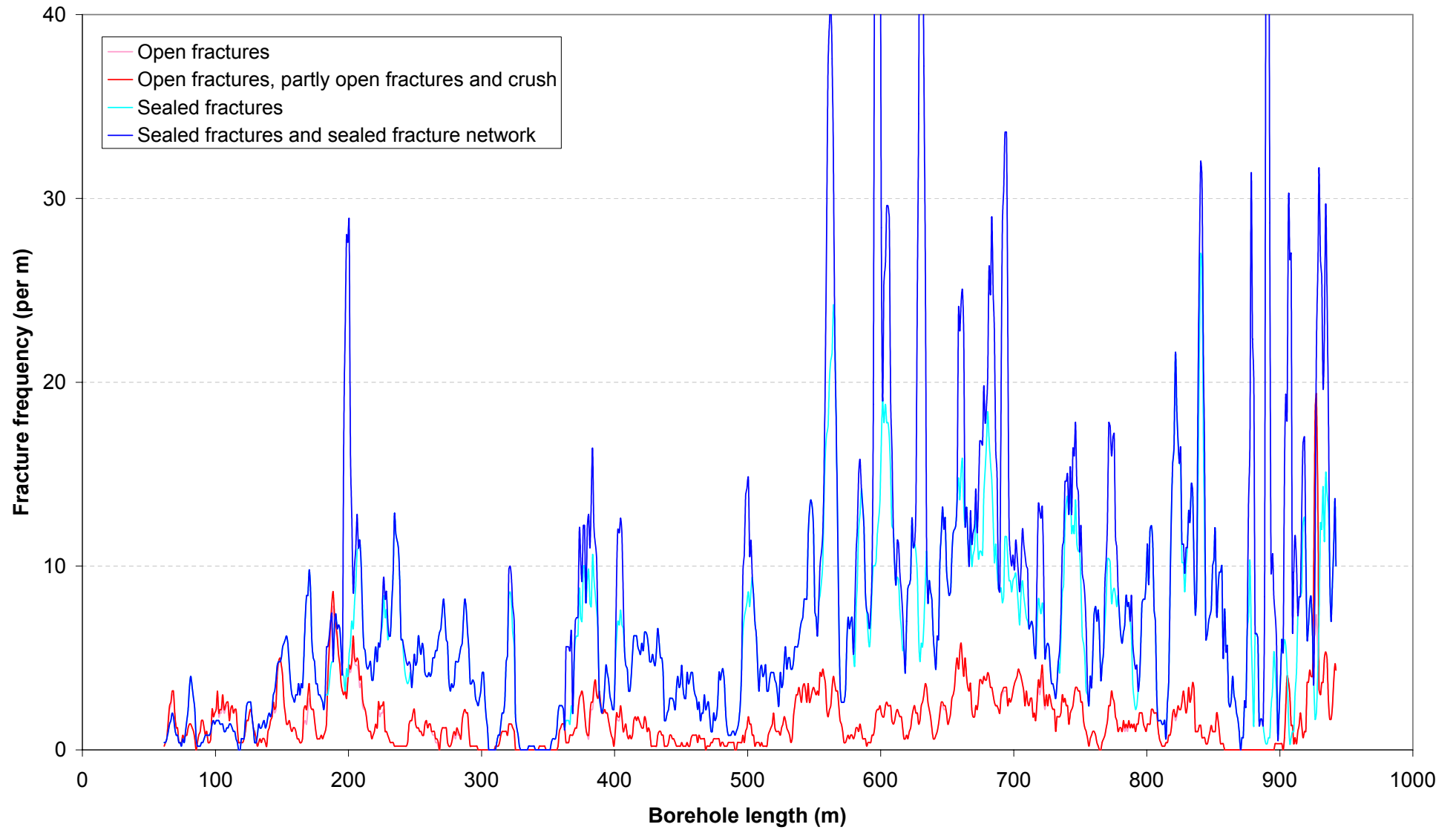


Figure 4-2. Terminology for brittle deformation zones (after /2/).

# KFM08D



17

Figure 4-3. Fracture frequency plot for KFM08D. Moving average with a 5 m window and 1 m steps.

The occurrence and orientation of radar anomalies within the possible deformation zones are used during the identification of these zones. An overview of the borehole radar measurement in KFM08D is shown in Figure 4-4. A conductive environment causes attenuation of the radar wave, which in turn decreases the penetration. The effect of attenuation can be observed in the borehole at 200 m, 360 m, 395 m, 550–650 m and at the bottom of the borehole (Figure 4-4). The effect of attenuation varies between the different antenna frequencies (20 MHz, 100 MHz, 250 MHz and 60 MHz directional antenna). In some cases, alternative orientations for oriented radar reflectors are presented. One of the alternatives is considered to be correct, but due to uncertainty in the interpretation of radar data, a decision concerning which of the alternatives that represent the true orientation cannot be made. Orientations from directional radar are presented as strike/dip using the right-hand-rule method.

### 4.2 Nonconformities

The section 927.98–942.30 m adjusted length in KFM08D was mapped without access to BIPS images.

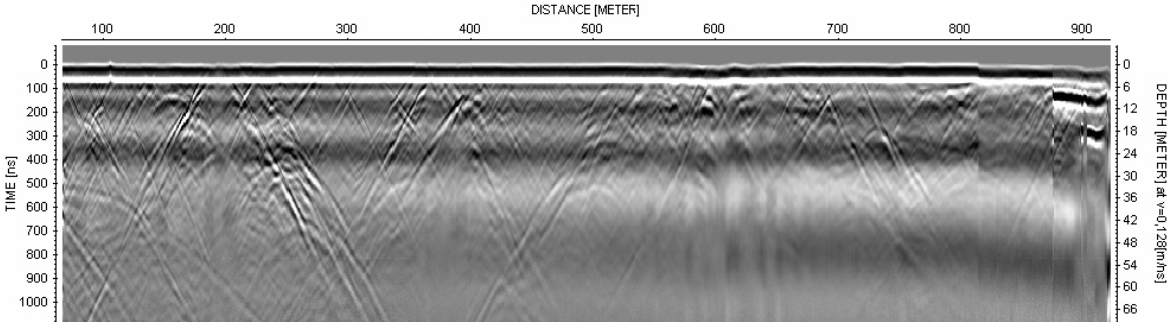


Figure 4-4. Overview (20 MHz data) of the borehole radar measurements in KFM08D.



## 5 Results

The results of the geological single-hole interpretation are presented as print-outs from the software WellCad (Appendix 1).

### 5.1 KFM08D

The borehole direction at the start is 100°/-55°.

#### **Rock units**

The borehole can be divided into five different rock units, RU1–RU5. Rock unit 2 occurs in three separate length intervals, rock unit 3 occurs in two separate length intervals and rock unit 4 occurs in two separate length intervals. The rock units have been recognized with a high degree of confidence.

#### **59.00–395.65 m**

RU1: Medium-grained metagranite-granodiorite (101057) with subordinate pegmatitic granite (101061), fine- to medium-grained metagranitoid (101051) and amphibolite (102017). Local occurrences of predominantly weak to medium albitization. Slightly higher frequency of open fractures outside possible deformation zones above 290 m with a tendency for an increase upwards. Several narrow resistivity anomalies outside possible deformation zones above 184 m. Confidence level = 3.

#### **395.65–569.76 m**

RU2a: Medium-grained metagranite-granodiorite (101057) with subordinate pegmatitic granite (101061), both generally affected by medium to weak albitization that corresponds to lower natural gamma radiation. Also subordinate fine- to medium-grained metagranitoid (101051) and amphibolite (102017). Confidence level = 3.

#### **569.76–597.00 m**

RU3a: Amphibolite (102017) and pegmatitic granite (101061). Medium albitization in the pegmatitic granite and locally chloritization in the amphibolite. Confidence level = 3.

#### **597.00–651.37 m**

RU4a: Heterogeneous unit with fine- to medium-grained metagranitoid (101051), pegmatitic granite (101061) and medium-grained metagranite-granodiorite (101057). The fine- to medium-grained metagranitoid (101051) shows a silicate density that corresponds to a tonalitic composition. Medium albitization in the pegmatitic granite and the medium-grained metagranite-granodiorite (101057) that corresponds to lower natural gamma radiation. Confidence level = 3.

#### **651.37–841.61 m**

RU2b: Medium-grained metagranite-granodiorite (101057) generally affected by medium to weak albitization that corresponds to lower natural gamma radiation. Subordinate pegmatitic granite (101061) and fine- to medium-grained granite (111058). Confidence level = 3.



### **841.61–876.71 m**

RU5: Fine- to medium-grained metagranitoid (101051) that shows a granodioritic tonalitic composition based on silicate density. Subordinate medium-grained metagranite-granodiorite (101057) that shows medium albitization, pegmatitic granite (101061) and amphibolite (102017). Confidence level = 3.

### **876.71–896.66 m**

RU4b: Heterogeneous unit with pegmatitic granite (101061), medium-grained metagranite-granodiorite (101057), fine- to medium-grained granite (111058), fine- to medium-grained metagranitoid (101051), and felsic to intermediate metavolcanic rock (103076). The fine- to medium-grained metagranitoid (101051) shows a silicate density that corresponds to a tonalitic composition. Generally medium to strong albitization with lower natural gamma radiation. Confidence level = 3.

### **896.66–928.52 m**

RU3b: Metadiorite (101033) with subordinate amphibolite (102017), fine- to medium-grained granite (111058) and pegmatitic granite (101061). Confidence level = 3.

### **928.52–941.75 m**

RU2c: Medium-grained metagranite-granodiorite (101057) generally affected by medium albitization. Subordinate pegmatitic granite (101061). Confidence level = 3.

### ***Possible deformation zones***

Twelve possible deformation zones have been recognised with different degree of confidence in KFM08D.

### **184–210 m**

DZ1: Increased frequency of sealed and open fractures, with some sealed fracture networks. Fractures that strike in the SW quadrant and dip steeply to the NW, and fractures that are gently dipping dominate. Steeply dipping fractures that strike NW-SE are also present. Apertures generally less than 1 mm and locally up to 8 mm. The most frequent fracture filling minerals are chlorite, calcite, adularia and pyrite. Low resistivity, P-wave velocity and magnetic susceptibility. Locally weak to medium oxidation. Twelve radar reflectors of which one is oriented (010/25). Zone situated in medium-grained metagranite-granodiorite with subordinate occurrences of pegmatitic granite and amphibolite. Confidence level = 2.

### **318–324 m**

DZ2: Increased frequency of predominantly sealed fractures. Gently dipping fractures and fractures that strike in the SW quadrant and dip steeply to the NW dominate. Apertures generally less than 1 mm. The most frequent fracture filling minerals are calcite, adularia and chlorite. No significant response in the geophysical logs. One radar reflector with an intersection angle of 39°. Zone situated in medium-grained metagranite-granodiorite with subordinate occurrences of pegmatitic granite and amphibolite. Confidence level = 1.

### **371–396 m**

DZ3: Increased frequency of predominantly sealed fractures. Fractures that strike in the SW quadrant and dip steeply to the NW, and fractures that are gently dipping dominate. Steeply dipping fractures that strike in the SE quadrant and dip moderately to steeply to the SW are also present. Apertures generally less than 1 mm. The most frequent fracture filling minerals are calcite, chlorite and adularia. Locally weak oxidation. Low resistivity below 385 m. Nine radar reflectors, one of which is strong, with intersection angles from 35–56°. Zone situated at the base of RU1 in medium-grained metagranite-granodiorite with subordinate occurrences of pegmatitic granite and metadiorite. Confidence level = 3.

### **496–506 m**

DZ4: Increased frequency of predominantly sealed fractures. Fractures show variable orientation. Fractures that strike in the SW quadrant and dip steeply to the NW are conspicuous. Apertures generally less than 1 mm. The most frequent fracture filling minerals are chlorite, calcite, laumontite and adularia. Low magnetic susceptibility and slightly reduced resistivity and P-wave velocity. Three radar reflectors, with intersection angles from 41–45°. Zone situated in albitized, medium-grained metagranite-granodiorite with subordinate occurrences of pegmatitic granite. Confidence level = 2.

### **546–571 m**

DZ5: Increased frequency of predominantly sealed fractures, with some sealed fracture networks. Fractures that strike in the SW quadrant and dip steeply to the NW dominate. Apertures generally less than 1 mm. The most frequent fracture filling minerals are chlorite, adularia, calcite, clay minerals and laumontite. Generally faint oxidation. Low magnetic susceptibility and slightly reduced resistivity and P-wave velocity. Eleven radar reflectors, with intersection angles from 7–85°. Zone situated at the base of RU2a and in albitized medium-grained metagranite-granodiorite with subordinate occurrences of pegmatitic granite and amphibolite. Confidence level = 3.

### **582–609 m**

DZ6: Increased frequency of predominantly sealed fractures, with some sealed fracture networks. Steeply dipping fractures that strike NNW-SSE and that show a variable strike in the SW quadrant dominate. Gently dipping fractures are also conspicuous. Apertures generally less than 1 mm and locally up to 3 mm. The most frequent fracture filling minerals are calcite, chlorite and quartz. Locally weak oxidation. Low magnetic susceptibility and minor resistivity and P-wave velocity anomalies. Four radar reflectors, with intersection angles from 51–62°. Zone situated on both sides of the boundary between RU3a and RU4a in amphibolite (RU3a) and fine- to medium-grained metatonalite (RU4a). Confidence level = 2.

### **621–634 m**

DZ7: Increased frequency of predominantly sealed fractures, with some sealed fracture networks. Steeply dipping fractures that strike SSE and dip to the WSW, and that strike WSW and dip to the NNW dominate. Gently dipping fractures are also conspicuous. Apertures generally less than 1 mm. The most frequent fracture filling minerals are calcite, chlorite and adularia. Locally weak oxidation. Low magnetic susceptibility and slightly reduced resistivity and P-wave velocity. Four radar reflectors, with intersection angles from 21–51°. Zone situated in fine- to medium-grained metatonalite and pegmatitic granite. Confidence level = 3.

#### **644–689 m**

DZ8: Increased frequency of sealed and open fractures, with some sealed fracture networks. Steeply dipping fractures that strike SSW and dip to the WNW, and that strike SSE and dip to the WSW dominate. Gently dipping fractures are also conspicuous. Apertures generally less than 1 mm, locally up to 2 mm. The most frequent fracture filling minerals are calcite, chlorite, quartz and adularia. Locally weak oxidation. Low magnetic susceptibility and slightly reduced resistivity. Fourteen radar reflectors of which three are oriented (161/67, 268/20 and 185/84). Zone situated at the top of RU2b in albitized medium-grained metagranite-granodiorite with subordinate fine- to medium-grained metatonalite and pegmatitic granite. Confidence level = 2.

#### **737–749 m**

DZ9: Increased frequency of predominantly sealed fractures. Steeply dipping fractures that strike NNE-SSW dominate. Gently dipping fractures are also present. Apertures generally less than 1 mm. The most frequent fracture filling minerals are calcite, chlorite and adularia. Low magnetic susceptibility and minor resistivity anomalies. Eleven radar reflectors of which one is oriented (080/21). Zone situated in albitized medium-grained metagranite-granodiorite. Confidence level = 2.

#### **770–777 m**

DZ10: Increased frequency of predominantly sealed fractures. Steeply dipping fractures that vary in strike between SSW-NNE and NNW-SSE dominate. Apertures generally less than 1 mm. The most frequent fracture filling minerals are laumontite, hematite and calcite. No significant response in the geophysical logs. Two radar reflectors with intersection angles 51° and 52° to borehole axis. Zone situated in albitized medium-grained metagranite-granodiorite with subordinate pegmatitic granite. Confidence level = 1.

#### **819–842 m**

DZ11: Increased frequency of predominantly sealed fractures. Steeply dipping fractures that vary in strike between NNE-SSW and NNW-SSE, and gently dipping fractures dominate. Apertures generally less than 1 mm, locally up to 1.5 mm. The most frequent fracture filling minerals are chlorite, adularia, quartz and calcite. Low magnetic susceptibility, one caliper anomaly and minor resistivity and P-wave velocity anomalies. Seven radar reflectors of which one is oriented (259/13). Zone situated at the base of RU2b in albitized medium-grained metagranite-granodiorite with subordinate fine- to medium-grained metatonalite and pegmatitic granite. Confidence level = 2.

#### **903–941.75 m**

DZ12: Increased frequency of sealed and open fractures. Some sealed fracture networks and a crush zone at 926 m are present. Sealed fractures show variable orientation. Open fractures are both gently and steeply dipping. The steeply dipping open fractures strike N-S and are sub-vertical, and strike SSW with a dip to the WNW. Apertures less than 1 mm. The most frequent fracture filling minerals are calcite, chlorite, clay minerals and quartz. Locally weak oxidation and at 923 to 929 m strong oxidation and chloritization. Quartz dissolution at 933.10 to 933.16 m. Two caliper anomalies, low magnetic susceptibility and resistivity, and locally low P-wave velocity. One prominent geophysical anomaly, including also increased natural gamma radiation between 924 m and 929 m. This is also seen as a prominent low amplitude section in the radar data. Seven radar reflectors with intersection angles of 3–55° to borehole axis. Zone situated in metadiorite, amphibolite, fine- to medium-grained granite, and albitized medium-grained metagranite-granodiorite. Confidence level = 3.

## 6 Comments


The results of the geological single-hole interpretation of KFM08D are presented in a WellCad plot (Appendix 1). The WellCad plot consists of the following columns:

- 1: Depth (length along the borehole)
- 2: Rock type
- 3: Rock alteration
- 4: Sealed fractures
- 5: Open and partly open fractures
- 6: Crush zones
- 7: Silicate density
- 8: Magnetic susceptibility
- 9: Natural gamma radiation
- 10: Estimated fracture frequency
- 11: Description: Rock unit
- 12: Stereogram for sealed fractures in rock unit (blue symbols)
- 13: Stereogram for open and partly open fractures in rock unit (red symbols)
- 14: Description: Possible deformation zone
- 15: Stereogram for sealed fractures in possible deformation zone (blue symbols)
- 16: Stereogram for open and partly open fractures in possible deformation zone (red symbols)

## References

- /1/ **Stephens M B, Lundqvist S, Bergman T, Andersson J, 2003.** Forsmark site investigation. Bedrock mapping. Rock types, their petrographic and geochemical characteristics, and a structural analysis of the bedrock based on Stage 1 (2002) surface data. SKB P-03-75, Svensk Kärnbränslehantering AB.
- /2/ **Munier R, Stenberg L, Stanfors R, Milnes A G, Hermanson J, Triumf C-A, 2003.** Geological site descriptive model. A strategy for the model development during site investigations. SKB R-03-07, Svensk Kärnbränslehantering AB.
- /3/ **Samuelsson E, Rauséus G, 2007.** Forsmark site investigation. Boremap mapping of telescopic drilled borehole KFM08D. SKB P-07-103, Svensk Kärnbränslehantering AB. (in prep.)
- /4/ **Mattsson H, Keisu M, 2007.** Forsmark site investigation. Interpretation of geophysical borehole measurements from KFM02B, KFM08D and KFM11A. SKB P-07-125, Svensk Kärnbränslehantering AB.
- /5/ **Gustafsson J, Gustafsson C, 2007.** Forsmark site investigation. RAMAC and BIPS logging in boreholes KFM02B and KFM08D. SKB P-07-96, Svensk Kärnbränslehantering AB.

# Geological single-hole interpretation of KFM08D

<b>Title</b> SINGLE HOLE INTERPRETATION KFM08D						
	<b>Site</b>	FORSMARK	<b>Inclination [°]</b>	-55.18	<b>Elevation [m.a.s.l.]</b>	2.61
	<b>Borehole</b>	KFM08D	<b>Date of mapping</b>	2007-01-18 09:05:00	<b>Drilling Start Date</b>	2006-11-23 09:00:00
	<b>Diameter [mm]</b>	77	<b>Coordinate System</b>	RT90-RHB70	<b>Drilling Stop Date</b>	2007-02-10 15:00:00
	<b>Length [m]</b>	942.300	<b>Northing [m]</b>	6700491.68	<b>Surveying Date</b>	
	<b>Bearing [°]</b>	99.98	<b>Easting [m]</b>	1631199.16	<b>Plot Date</b>	2007-06-25 23:44:05
<b>Signed data</b>						

<b>ROCKTYPE FORSMARK</b>		<b>ROCK ALTERATION</b>		<b>SILICATE DENSITY</b>		<b>SUSCEPTIBILITET</b>		<b>NATURAL GAMMA</b>	
Granite, fine- to medium-grained	Oxidized	unclassified	unclassified	dens<2680 (Granite)	sus<0.001	gam<20	gam<20	20<gam<36	36<gam<53
Pegmatite, pegmatitic granite	Chloritized	2680<dens<2730 (Granodiorite)	sus<0.01	2730<dens<2800 (Tonalite)	0.01<sus<0.1	20<gam<36	20<gam<36	36<gam<53	36<gam<53
Granite, granodiorite and tonalite, metamorphic, fine- to medium-grained	Epidotitized	2800<dens<2890 (Diorite)	0.01<sus<0.1	dens>2890 (Gabbro)	0.01<sus<0.1	20<gam<36	20<gam<36	36<gam<53	36<gam<53
Granite, metamorphic, aplitic	Albitization	Laumontitization	0.01<sus<0.1			36<gam<53	36<gam<53	36<gam<53	36<gam<53
Granite to granodiorite, metamorphic, medium-grained	Saussuritization								
Diorite, quartz diorite and gabbro, metamorphic	Laumontitization								
Amphibolite									
Felsic to intermediate volcanic rock, metamorphic									

